

Giant room-temperature magnetocapacitance in Co^{2+} doped SnO_2 dielectric films

Jian-guo Wan,^{a)} Qi Lu, Bo Chen, Fengqi Song, Jun-ming Liu, Jingbing Dong, and Guanghou Wang

Department of Physics and National Laboratory of Solid State Microstructures, Nanjing University, Nanjing 210093, People's Republic of China

(Received 1 September 2009; accepted 23 September 2009; published online 14 October 2009)

The giant room-temperature magnetocapacitance is reported in the Co^{2+} substitutionally doped SnO_2 film in which the ferromagnetism coexists with the dielectric state. The maximum magnetocapacitance is observed in the $\text{Sn}_{0.98}\text{Co}_{0.02}\text{O}_2$ film in which the magnetocapacitance is as large as 0.45 at frequency of 1.0 kHz and saturated magnetic field of ~ 6.0 kOe. We experimentally demonstrate that such magnetocapacitance effect correlates with the Co dopant concentration and the existence of oxygen vacancy. The electric polarization response of the oxygen vacancy–Co ion complexes to the magnetic field is attributed to the origin of the magnetocapacitance. © 2009 American Institute of Physics. [doi:10.1063/1.3249584]

The modulation of capacitance by an external magnetic field excitation, namely magnetocapacitance (MC) effect, has been attracting an intense interest due to its potential and important applications in the next-generation electronic devices such as tunable spin filters, magnetic sensors, storage devices, etc.^{1–6} Some efforts have been made to search MC effect in several material systems, such as the multiferroic compounds (e.g., LuFe_2O_4),¹ the spin tunneling junction (e.g., $\text{Co}/\text{Al}_2\text{O}_3/\text{Co}$),² the double perovskite film (e.g., $\text{La}_2\text{CoMnO}_6$),³ etc. However, most of them only show weak MC effect at cryogenic temperature, which are not suitable for the practical applications.

On the other hand, in recent years, the dilute magnetic oxides such as ZnO and TiO_2 doped with transition-metal (TM) ions have been becoming a hot topic due to their attractive multifunctionality.⁷ In general, they exhibit semiconductivity as well as room-temperature ferromagnetism because of the coupling interaction between the free charge carriers and spins.⁸ Recently, Griffin *et al.*⁹ experimentally demonstrated that the presence of free carriers was not required for the room-temperature ferromagnetism in some TM-doped oxides with “bad quality.” They were thus called as “dilute magnetic dielectrics (DMDs)” because the ferromagnetism can coexist with the highly insulating dielectric state. The indirect interaction between the oxygen vacancies and doped TM ions are demonstrated to be responsible for the formation of ferromagnetic orders.¹⁰ In this sense, the application of external magnetic field to such DMD system may induce the spin-related coupling interaction between the electron charges, oxygen vacancies, and doped ions, consequently leading to all kinds of magnetoelectric coupling process, e.g., MC effect. In this letter, we report the giant room-temperature MC in the Co^{2+} substitutionally doped SnO_2 film with highly insulating dielectric state, which has been not reported previously and shows potential for the practical applications. The origin of the MC in this DMD film is proposed.

The Co ion doped SnO_2 nanocrystalline colloids with average diameter of ~ 3 nm were first prepared by a hydrothermal reaction route in an inverse micelle system of $\text{Sn}^{4+}/\text{Co}^{2+}$ aqueous solution/oleic acid at 150 °C for 12 h. The Co dopant concentration was set in the range of $0 < x < 0.10$. Subsequently, the $\text{Sn}_{1-x}\text{Co}_x\text{O}_2$ film was prepared by spin coating the nanocrystalline colloids onto the Pt/Ti/SiO₂/Si(100) wafer, and then annealed at 600 °C for 5 min under the N₂ atmosphere. The final film was ~ 200 nm in thickness. The experimental details could be found in our previous work.¹¹ The x-ray diffraction, x-ray photoelectron spectroscopy, and specific ligand-field absorption spectra measurements on the films confirmed that the Co^{2+} ions were substitutionally doped at Sn^{4+} sites in SnO_2 and no metallic Co clusters or other Co phases exists in the sample except for the rutile SnO_2 structure. Figure 1 presents the room-temperature in-plane magnetic hysteresis loops for the $\text{Sn}_{1-x}\text{Co}_x\text{O}_2$ films with various x measured on a superconducting quantum interference device. All films exhibit well-defined ferromagnetic behaviors. The saturation magnetization increases with increasing x , till reaches the maximum value of $0.27 \mu_B/\text{Co}^{2+}$ at $x=0.02$, and then drops (inset of Fig. 1).

For electric measurement, Pt electrodes with 0.2 mm diameter were deposited on the film surface by pulsed laser

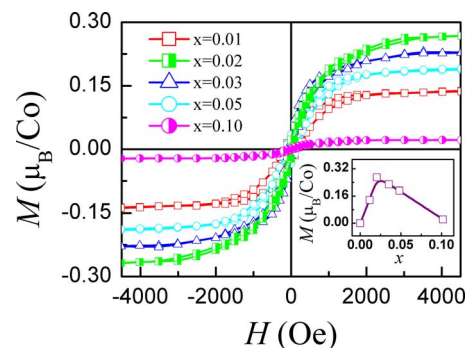


FIG. 1. (Color online) Room-temperature in-plane magnetic hysteresis loops of the $\text{Sn}_{1-x}\text{Co}_x\text{O}_2$ films with various x . The inset is the variation of saturation magnetization with x .

^{a)} Author to whom correspondence should be addressed. Electronic mail: wanjg@nju.edu.cn.

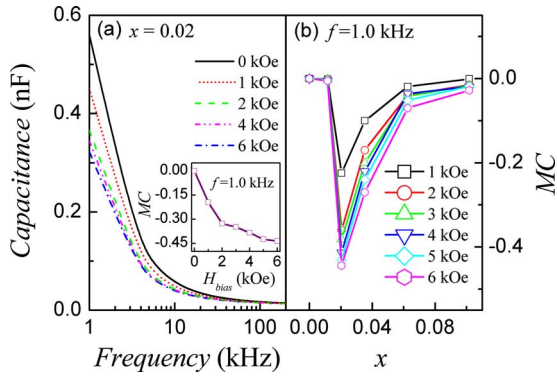


FIG. 2. (Color online) (a) Frequency dependence of capacitance under various H_{bias} at room temperature for the typical $\text{Sn}_{1-x}\text{Co}_x\text{O}_2$ film with $x=0.02$. The inset is its capacitance as a function of H_{bias} measured at $f=1.0$ kHz. (b) The x dependence of MC under various H_{bias} measured at $f=1.0$ kHz.

deposition. All films exhibited very high resistivity value beyond $\sim 1 \times 10^{10} \Omega \text{ cm}$ at zero field, which enables us to further explore their dielectric response to the magnetic field. Figure 2(a) presents the frequency dependence of room-temperature capacitance at various magnetic bias (H_{bias}) for the typical $\text{Sn}_{0.98}\text{Co}_{0.02}\text{O}_2$ film. The capacitance rapidly decreases with increasing frequency, and gradually reaches a stable constant as the frequency is beyond ~ 100 kHz. More interestingly, one observes that the capacitance strongly depends on the H_{bias} . Provided the MC is defined as $\text{MC} = 100\% \times [C(H) - C(0)]/C(0)$, where $C(H)$ and $C(0)$ represent the capacitance at H_{bias} and zero magnetic bias respectively, the H_{bias} dependence of MC can be plotted, as shown in the inset of Fig. 2(a). The negative MC value rapidly decreases with increasing H_{bias} and falls to a stable value near the saturated magnetic bias of $H_{\text{bias}} \sim 6.0$ kOe, indicating that strong magnetodielectric coupling happens in the film. We then measured the MC variation with x at fixed frequency of $f=1.0$ kHz under various H_{bias} , as shown in Fig. 2(b). The MC for all samples are unanimously negative, decrease sharply with increasing x , until it reaches the lowest point at $x \sim 0.02$, and then increases. At $x \sim 0.02$, the saturation value of $|\text{MC}|$ is as large as 0.45 at $H_{\text{bias}}=6.0$ kOe. Such giant room-temperature MC is surprising, substantially larger than all of the reported values in the other material systems (generally several percent points which only occur at low temperature),²⁻⁶ and even larger than that of LuFe_2O_4 bulk (about ~ 0.25 at $H_{\text{bias}}=1.0$ kOe measured at room temperature).¹

In order to explore the origin of MC effect in the present $\text{Sn}_{1-x}\text{Co}_x\text{O}_2$ films, we further studied their microstructure characteristics. The room-temperature electron paramagnetic resonance (EPR) spectra were first measured to examine whether there existed the oxygen vacancies in the films, as shown in Fig. 3. No EPR signal was detected when the sample had no Co dopant or the $\text{Sn}_{1-x}\text{Co}_x\text{O}_2$ film was not subjected to the annealing treatment. However, with annealing in the N_2 atmosphere at 600°C , the remarkable EPR signal appears. Moreover, the EPR signal significantly varies with the Co concentration and reaches the strongest at $x=0.02$. We further calculated the Lande factor g from the EPR spectra and found that the g value for all samples is ~ 2.0036 . This indicates that the EPR signal originates from the oxygen vacancies.^{12,13} In fact, benefited from the nanocrystalline colloids derived from the chemical preparation

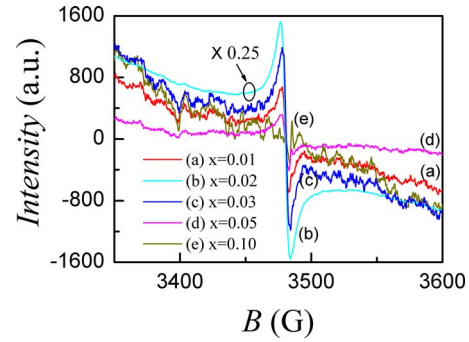


FIG. 3. (Color online) EPR spectra of the $\text{Sn}_{1-x}\text{Co}_x\text{O}_2$ films with various x .

process as well as the annealing treatment under the N_2 atmosphere, a great deal of oxygen vacancies were created in the $\text{Sn}_{1-x}\text{Co}_x\text{O}_2$ film due to the absence of oxygen.⁹

The existing state of the oxygen vacancies is crucial for the response of the samples to the external magnetic field. So we further carried out the microarea Raman spectroscopy measurement to explore the existing state of the oxygen vacancies. Figure 4(a) presents the Raman spectra of the films with various x . Two vibrational modes located at 637 and 784 cm^{-1} are observed, which are attributed to the classic SnO_2 vibrations.¹⁴ Addition of Co results in the appearance of two new bands at 607 and 723 cm^{-1} , which should be assigned to the local vibrational modes activated by local structural changes resulting from the substitution of Co^{2+} ions at the Sn^{4+} sites.¹⁵ Actually, since the mass of Co is lower than the mass of Sn, the local vibrational mode associated with the substitutional Co^{2+} in the SnO_2 lattice (i.e., the disordered $-\text{Co}-\text{O}-\text{Sn}-$ vibrational mode) is expected at higher frequency, which can be estimated using the mass defect equation¹⁶

$$\omega = \omega_M \left(\frac{1 - f\varepsilon}{1 - \varepsilon} \right)^{1/2}, \quad (1)$$

where ω_M is the maximum frequency of the TO phonons of SnO_2 (here $\omega_M=637 \text{ cm}^{-1}$), $\varepsilon=1-M_{\text{Co}}/M_{\text{Sn}}=0.50$, and f is the relative value of optical and acoustical phonon density of states (here $f=0.72$, which is similar to the TiO_2 system). From Eq. (1), the local $-\text{Co}-\text{O}-\text{Sn}-$ vibrational mode is expected at 721 cm^{-1} , which is almost consistent with the measured Raman band of 723 cm^{-1} .

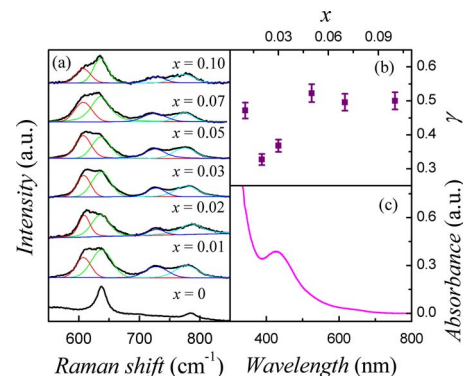
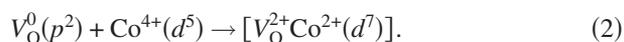


FIG. 4. (Color online) (a) Raman spectra and Lorentzian dividing and fitting of the $\text{Sn}_{1-x}\text{Co}_x\text{O}_2$ films with various x . (b) Vibrational intensity ratio γ of the $-\text{Co}-\text{O}-\text{Sn}-$ band at 723 cm^{-1} to the $-\text{Sn}-\text{O}-\text{Sn}-$ band at 637 cm^{-1} as a function of x . (c) Specific ligand-field absorption spectra of the $\text{Sn}_{0.98}\text{Co}_{0.02}\text{O}_2$ film.

Figure 4(b) further gives the vibrational intensity ratio (γ) of the $-\text{Co}-\text{O}-\text{Sn}-$ band at 723 cm^{-1} to the $-\text{Sn}-\text{O}-\text{Sn}-$ band at 637 cm^{-1} at various x . For the calculation of the vibrational intensity, all peaks for each Raman spectra were fitted by using the standard Lorentzian fitting method. One observes that, the γ value decreases with increasing x , reaches the minimum near $x \sim 0.02$, and then increases to a stable value. Combined with the EPR results that the maximum concentration of oxygen vacancy appears at $x \sim 0.02$, we accordingly infer that the existence of oxygen vacancies suppress the vibration of $-\text{Co}-\text{O}-\text{S}-$ band. That is to say, the oxygen vacancies are captured by the Co^{2+} ions and further interact with the Co^{2+} ions. This process can be described by the Kikoin's theoretical model for the TM-doped DMD oxide in which the oxygen vacancy (V_{O}) tends to be captured by the Co^{2+} ions to form the complex $[\text{V}_{\text{O}}^{2+}\text{Co}^{2+}]$ based on the charge transfer reaction¹⁰



As a result, the additional ferromagnetic orders are generated due to the superexchange between the $[\text{V}_{\text{O}}^{2+}\text{Co}^{2+}]$ complexes where the Co^{2+} ions exchange electrons via empty vacancy level. For the present $\text{Sn}_{1-x}\text{Co}_x\text{O}_2$ film, such electron transfer in the complexes can be further experimentally confirmed by the ligand-field absorption spectra [shown in Fig. 4(c)], in which the strong shoulder peak at $\sim 420\text{ nm}$ is ascribed to the absorption of trapped electrons by Co^{2+} ions since the metal centers can act as the electron traps.¹¹

From above experimental results and analyses, we have some idea about the origin of the MC effect in the present $\text{Sn}_{1-x}\text{Co}_x\text{O}_2$ DMD films as follows. During the charge transfer reaction in the $[\text{V}_{\text{O}}^{2+}\text{Co}^{2+}]$ complexes, the system remains highly insulating because the vacancy-related electrons are still bound by Co^{2+} ions. The dielectric response of the system significantly depends on this unique spin texture,⁶ i.e., the configuration of the $[\text{V}_{\text{O}}^{2+}\text{Co}^{2+}]$ complexes, which possess both ferromagnetic orders and highly insulating dielectric state. Under the external magnetic field, the response of the ferromagnetic orders in the complexes induces the electric charges in the complexes to deviate from their symmetry center, consequently leading to the induced polarized electric charges. Obviously, this polarized electric charges under the magnetic field significantly depends on the oxygen vacancy

concentration in the system. So it is understandable that the MC is maximum for the $\text{Sn}_{0.98}\text{Co}_{0.02}\text{O}_2$ film in which the oxygen vacancy concentration is maximum.

In summary, the giant room-temperature MC in the Co^{2+} substitutionally doped SnO_2 films is observed. The experimental results demonstrate that the MC effect is related to the Co dopant concentration and oxygen vacancy. The electric polarization response of the oxygen vacancy-Co ion complexes to the external magnetic field is attributed to the MC effect.

This work was supported by the National Natural Science Foundation of China (Grant Nos. 10774070 and 90606002), the Provincial Nature Science Foundation of Jiangsu in China (Grant No. BK2008024), the National Key Projects for Basic Research of China (Grant Nos. 2010CB923401 and 2009CB623303), and the Program for New Century Excellent Talents in University of China (Grant No. NCET-07-0422).

¹M. A. Subramanian, T. He, J. Z. Chen, N. S. Rogado, T. G. Calvarese, and A. W. Sleight, *Adv. Mater.* **18**, 1737 (2006).

²H. Kaiju, S. Fujita, T. Morozumi, and K. Shiiki, *J. Appl. Phys.* **91**, 7430 (2002).

³M. P. Singh, K. D. Truong, and P. Fournier, *Appl. Phys. Lett.* **91**, 042504 (2007).

⁴N. Hur, S. Park, S. Guha, A. Borissov, V. Kiryukhin, and S.-W. Cheong, *Appl. Phys. Lett.* **87**, 042901 (2005).

⁵M. P. Singh, W. Prellier, C. Simon, and B. Raveau, *Appl. Phys. Lett.* **87**, 022505 (2005).

⁶M. Gich, C. Frontera, A. Roig, J. Fontcuberta, E. Molins, N. Bellido, C. Simon, and C. Fleta, *Nanotechnology* **17**, 687 (2006).

⁷S. A. Chambers, *Surf. Sci. Rep.* **61**, 345 (2006).

⁸S. J. Pearton, C. R. Abernathy, D. P. Norton, A. F. Hebard, Y. D. Park, L. A. Boatner, and J. D. Budai, *Mater. Sci. Eng. R.* **40**, 137 (2003).

⁹K. A. Griffin, A. B. Pakhomov, C. M. Wang, S. M. Heald, and K. M. Krishnan, *Phys. Rev. Lett.* **94**, 157204 (2005).

¹⁰K. Kikoin and V. Fleurov, *Phys. Rev. B* **74**, 174407 (2006).

¹¹D. Y. Pan, J. G. Wan, G. L. Xu, L. Y. Lv, Y. J. Wu, H. Min, J. M. Liu, and G. H. Wang, *J. Am. Chem. Soc.* **128**, 12608 (2006).

¹²M. Sterrer, E. Fischbach, T. Risse, and H.-J. Freund, *Phys. Rev. Lett.* **94**, 186101 (2005).

¹³S. L. Zhang, W. Li, Z. S. Jin, and Z. J. Zhang, *J. Solid State Chem.* **177**, 1365 (2004).

¹⁴J. Hays, A. Punnoose, R. Baldner, M. H. Engelhard, J. Peloquin, and K. M. Reddy, *Phys. Rev. B* **72**, 075203 (2005).

¹⁵C. Sudakar, P. Kharel, G. Lawes, R. Suryanarayanan, R. Naik, and V. M. Naik, *J. Phys.: Condens. Matter* **19**, 026212 (2007).

¹⁶X. Mathew, J. Hays, C. Mejia-Garcia, G. Contreras-Puente, and A. Punnoose, *J. Appl. Phys.* **99**, 08M101 (2006).